3-6-3 Beam Forming Network

MATSUMOTO Yasushi and IDE Toshiyuki

A newly developed BFN (Beam Forming Network) for a phased array feed on ETS-VIII satellite is described. The BFN controls the excitation weight of the feed arrays, which are located at a defocus position of the large deployable reflector antennas. The BFN described here has a unique architecture by which excitation weight for beam steering can be sheared by multiple beams. This enables simple and effective calibration of beam pointing errors caused by mechanical, thermal, or electrical environment in satellite orbit. The BFN also has a self-calibration function to reduce excitation weight errors caused by thermal environment.

Keywords

Phased array antenna, Satellite antenna, Beam forming network, Multi beam antenna, Satellite communications

1 Introduction

In order to establish a direct voice communication link in the S-band between handheld terminals and a geostationary satellite [1]-[3], the satellite must feature an antenna with an aperture diameter of 10 m or more, which is deployable in satellite orbit. Such antennas will have very narrow antenna beams, and will entail the accurate pointing of multiple antenna beams to cover desired service areas. The onboard antenna system presents a number of technical challenges involving (among others) reflector structure, the architecture of the feed system, the beam-forming method, antenna pointing method, and reduction in the weight and size of the antenna system.

In the ETS-VIII onboard antenna, the feed array is “defocused” toward the reflector at a certain distance from the focal plane of the deployable antenna reflector. Beam forming and pointing control are carried out mainly by changing the phase of the feeding signal, in what is referred to as a phased-array-fed system [3]-[5]. This method offers the following advantages (1) the degree of freedom in beam formation is high, with redundancy ensured in the event of failures of individual array elements or of the feed system; (2) in the transmitting antenna system, problems associated with the electrical overload on the feed section can be mitigated through the use of a spatial power combine with multiple radiating elements; and (3) allocation of onboard power resource to antenna beams can be dynamically optimized according to the regional traffic demand without changing the driving levels of the power amplifiers, by sharing the excitation amplitude distributions of the feed array among beams.

On the other hand, it is important to excite the feed array in a highly precise manner in order to secure the area gain required in a multibeam satellite communication system (i.e., the minimum gain required for a given area) and to ensure beam isolation (measured as the ratio of the main-lobe gain of a given beam to the side-lobe level of another beam using the same frequency). Moreover, since a large number of feed elements are used in beam formation, the scale of the BFN circuit increases along with an increase in the number of beams and feed elements. Therefore, the important technical challenges will consist of

ensuring excitation accuracy and maintaining simplicity and compact size in the BFN hardware.

The ETS-VIII will carry two kinds of BFNs (BFN1, BFN2) designed to address these technical challenges, each using a different approach [3]. BFN1 embodies a uniform pointing control system [6], the result of simplification of the pointing control method. The BFN2, on the other hand, applies highly integrated large-scale MMIC technology to establish independent pointing control for all beams [7]. The BFN1 and BFN2 have been developed by Communications Research Laboratory and NTT, respectively.

This paper describes the BFN1 the BFC (Beam Forming Controller). Based on the fact that pointing errors for multiple beams which share an antenna reflector are caused by many common factors, the BFN1 for the transmitting antenna has been designed to correct these common pointing errors uniformly, with shared variable attenuators and shared phase shifters. This method (uniform pointing control method) can greatly reduce the number of control weights for pointing control, and can simplify the control algorithm for beam pointing. The BFC compensates for fluctuations in array weight through onboard calculation, in response to temperature changes in the onboard equipment, in addition to its various functions in beam-pointing experimentation.

Below we will describe an outline of the satellite's onboard beam-forming section; the structures, functions, and performance of the BFN1 and the BFC; and the beam scanning performance of the antenna.

2 Outline of phased-array-fed system and beam forming section

The ETS-VIII satellite carries two phased-array-fed large deployable reflector antennas, dedicated to transmission and reception, respectively [8][9]. The antenna reflector is an offset parabola consisting of fourteen hexagonal deployment modules. A feed array, in which thirty-one cup MSA (microstrip) elements [10] are arranged in a triangle is displaced toward the reflector by a given defocus distance from the focal plane of the reflector. The position of the feed array, the number of elements, element arrangement, and excitation weight are designed to optimize [9] antenna performance. In the transmission system, the excitation amplitude distribution of the array is shared, so that the transmitting power can be freely allocated to multiple beams.

The beam forming section features two kinds of beam-forming networks (BFN1 and BFN2), for transmission and reception respectively, each of which can form three beams. The uniform pointing control method with shared weight is applied to two beams of the transmitting BFN1. This method is theoretically applicable to both transmission and reception, but the receiving BFN1 is operated by independent pointing control, for the following reasons. In the transmission system, the excitation amplitude distribution of the array is shared by multiple beams, which is more compatible with the uniform pointing control method because both the excitation amplitude and the phase are controllable in common. On the other hand, the receiving antenna is required to have greater beam isolation than the transmitting antenna. This is because one must consider the situation that the uplink signals are attenuated by fading, whereas uplink interfering signals from frequency-shared areas do not suffer attenuation. Moreover, the link margin is less in the uplink between the ETS-VIII and a handheld terminal than that in the down link [11]. Therefore, it is best to individually optimize the array weight of each beam.

The excitation weight of the transmitting/receiving BFN1 is controlled by the beam-forming controller (BFC). In order to avoid a critical problem that a single failure in the built-in processor may cause the loss of the beam forming function, two BFC components are equipped separately on the satellite to configure a cold standby system.

Fig.1 shows an example of the beam allo-

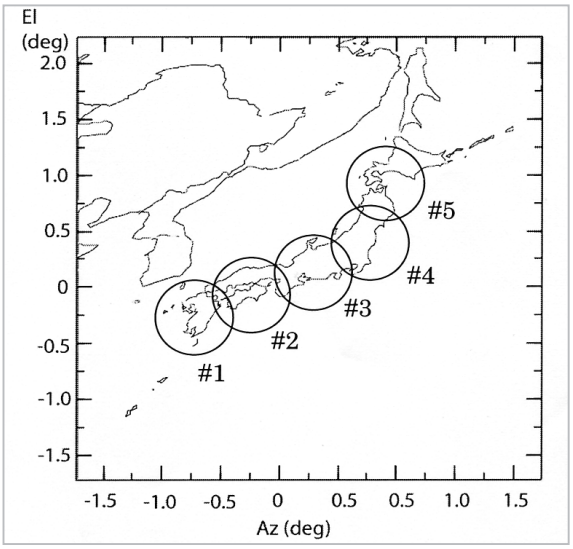

Fig.1 *Beam allocation for mobile communications.*

cation for multi-beam mobile communication. Each circle indicates a beam position corresponding to an area gain of 42 dBi. The same frequencies are re-used for beam positions #1 and #4 and for beam positions #2 and #5, respectively. Of the five beam positions indicated in the figure, the uniformly pointing-controlled beams correspond to beam positions #3 and #4 among the three beams formed by the transmitting BFN1. On the other hand, the independently controlled beam is formed at an arbitrary beam position. Moreover, when carrying out broadcast experiments, the array weight of the independently controlled beam is modified to form a single dedicated beam.

3 Functions of BFN and beam scanning method

The functional block diagram of the transmitting BFN1 and the receiving BFN1 are shown in Fig.2. In the transmitting BFN, the input signals to the uniformly pointing-controlled beams (to beam ports 2 and 3 in Fig.2a) are output to the element ports through the shared variable attenuators and the shared phase shifters shown in the figure. The shared attenuators and phase shifters are used for correction of the excitation error produced by factors such as temperature changes in the com-

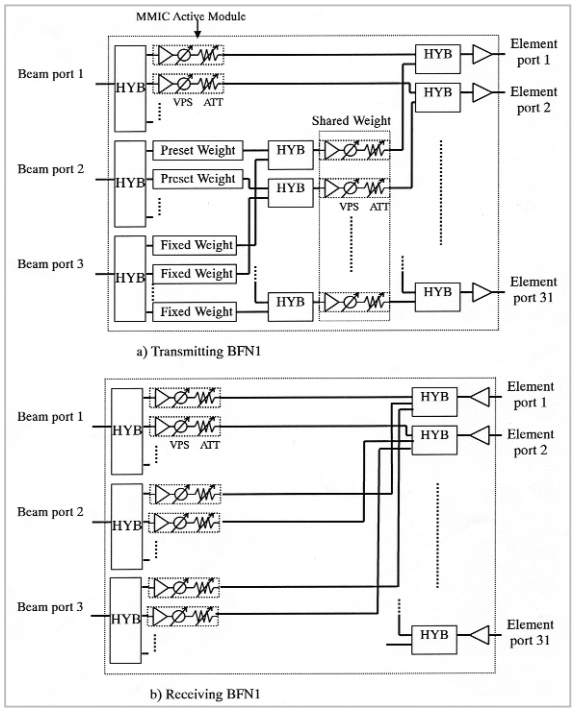

Fig.2 *Architecture of the BFN1. ATT:Variable attenuator, VPS:Variable phase shifter, HYB:Hybrid circuit a)Transmitting BFN1, b)Receiving BFN1*

ponents of the feed system which are shared by the beams (e.g., power amplifiers, filters, and feed lines in the transmitting feed section). Moreover, beam pointing errors caused by common mechanical factors (satellite attitude error, alignment error of feed-elements, alignment error of the reflector after deployment, or reflector distortion, for example) are corrected by antenna beam scanning, using the shared phase shifters.

In Fig.3, the phase shift ξ_n of element n

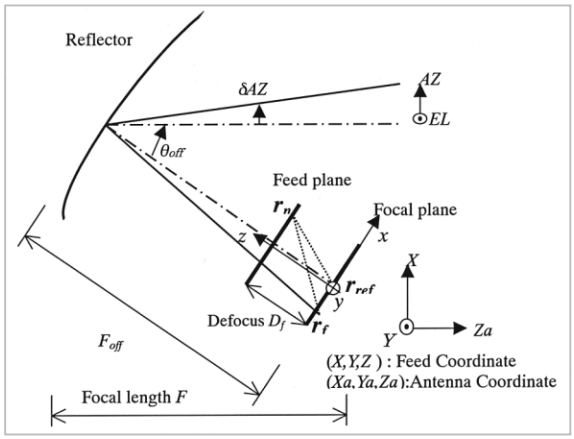

Fig.3 *Coordinate systems of a phased-array-fed reflector antenna.*

necessary to scan in a direction (in units of [rad]) from (AZ, EL) to (AZ + δAZ, EL + δ EL) is expressed by the following formula, in which virtual feed positions on the focal plane before and after scanning are designated as r_f and r_{ref} [6].

$$\xi_n = k(|r_n - r_f| - |r_f - r_{ref}|) \quad (1)$$

$$\fallingdotseq k(F_{off}/D_f)(X_n \cdot \delta AZ - Y_n \cdot \delta EL), \quad (2)$$

where

$k=2\pi/\lambda$

$r_n=(X_n,Y_n,D_f)$: element position (n=1 to N),

$r_{ref}=(X_{ref},Y_{ref},Z_{ref})=(-F_{off}\cdot\tan(AZ),F_{off}\cdot\tan(EL),0)$,

$r_f=(X_f,Y_f,Z_f)=(-F_{off}\cdot\tan(AZ+\delta AZ),F_{off}\cdot\tan(EL+\delta EL),0)$,

(δAZ, δEL): beam scan angle [rad]

$F_{off}=F/\cos^2(\theta_{off}/2)$: distance between the aperture center and the focal point,

F: focal length of the reflector,

Df: defocus distance, and

θ_{off} : reflector offset angle.

Equation (2) indicates that the phase shift does not depend on the initial direction and that beams with different directions can be scanned jointly. The phase shift with respect to a unit scan angle becomes F_{off}/D_f times the phase shift of the direct radiation array.

In a phased-array-fed reflector antenna, as the scan angle from a boresight increases, directivity is generally degraded due to aberration, a phenomenon not seen in a direct radiation array. In some cases the scan angle used in Eq.(2) (referred to as the "steering angle in Eq.(2)") may not necessarily agree with the actually obtained scan angle. Furthermore, for a shaped antenna beam that has been formed under gain constraint (in order to secure sufficient area gain and beam isolation), it is difficult to define the beam scan angle using the direction in which the antenna gain is maximum. In this paper, desired scan angles (δ AZ', δEL') are defined using an area in which the gain constraints are imposed, and the steering angles (δAZ', δEL') to be substituted into Eq.(2) are determined as follows.

1) Areas of constraint are defined within which area gain or beam isolation must be ensured, with array weight optimized accordingly (referred to as the "initial array weight"). The obtained excitation phase is designated as η_n (n = 1 to N).
2) All constraint areas are translated by desired scan angles (δAZ, δEL) [rad], and the excitation phase η'_n is obtained similarly as in step 1). The difference in excitation phase before and after scanning is designated as $\delta\eta_n = \eta'_n - \eta_n$.
3) Determine the phase gradients Nx, Ny to be the best fit to the distribution of the phase difference of $\delta\eta_n$ on the feed plane by minimizing the square phase deviation ε^2. Here, in order to avoid the phase ambiguity of 2π, ε^2 is defined by the following formula (the range of the function arg (*) is set between $-\pi$ and π).

$$\varepsilon^2 = \sum \arg^2 [\exp(jk(X_n \cdot N_x - Y_n \cdot N_y + C) - j\delta\eta_n)] \quad (3)$$

4) The steering angle to be substituted into Eq.(2) is determined as follows.

$$\delta AZ = D_f / F_{off} \cdot \sin^{-1}(N_x),\ \delta EL = D_f / F_{off} \cdot \sin^{-1}(N_y)\ [\text{rad}] \quad (4)$$

Next, numerical calculation was performed based on the specifications of the antennas equipped on ETS-VIII. Since the excitation amplitude distribution for transmission is a specified constant regardless of the direction of beam pointing, only the phase optimization was carried out. The conditions of constraint consist of an area gain of 42 dBi or more and a beam isolation of 27 dB or more (equivalent to gain of 15 dBi or less). Although the specification value for beam iso-

lation of the transmitting antenna is 20 dB or more, the constraint condition was set more strictly in order to allow for degradation due to excitation errors (weight optimization is performed based on the assumption of no excitation errors).

Fig.4 a) shows an example of the obtained antenna pattern. In the figure, the five points in the Tokai area indicate constraint points for area gain, and the five points in the Kyushu area indicate the constraint points for beam isolation. The gain contour line of 42 dBi corresponds to the constraint value for area gain, and the contour line of 15 dBi corresponds to the constraint value for beam isolation. Fig.4 b) shows a pattern optimized by translating all constraint points, with the desired scan angle set to 0.5 degrees in the EL direction. Fig.4 c) shows the pattern obtained by scanning the beam using Eqs. (2) and (4) on the initial array weight. Comparing Fig.4 b) with Fig.4 c), the contours corresponding to the area gain and beam isolation in Fig.4c) nearly agrees with those in Fig.4b). In both Fig.4 b) and c), the areas in which the required beam isolation is obtained become narrower than the corresponding area in Fig.4 a). This is attributed to the increase in the scan angle from the boresight of the main lobe. In actual geostationary orbit, there is little probability that antenna pointing error will exceed 0.5 degrees due to satellite attitude error and/or thermal deformation of the reflecting surface.

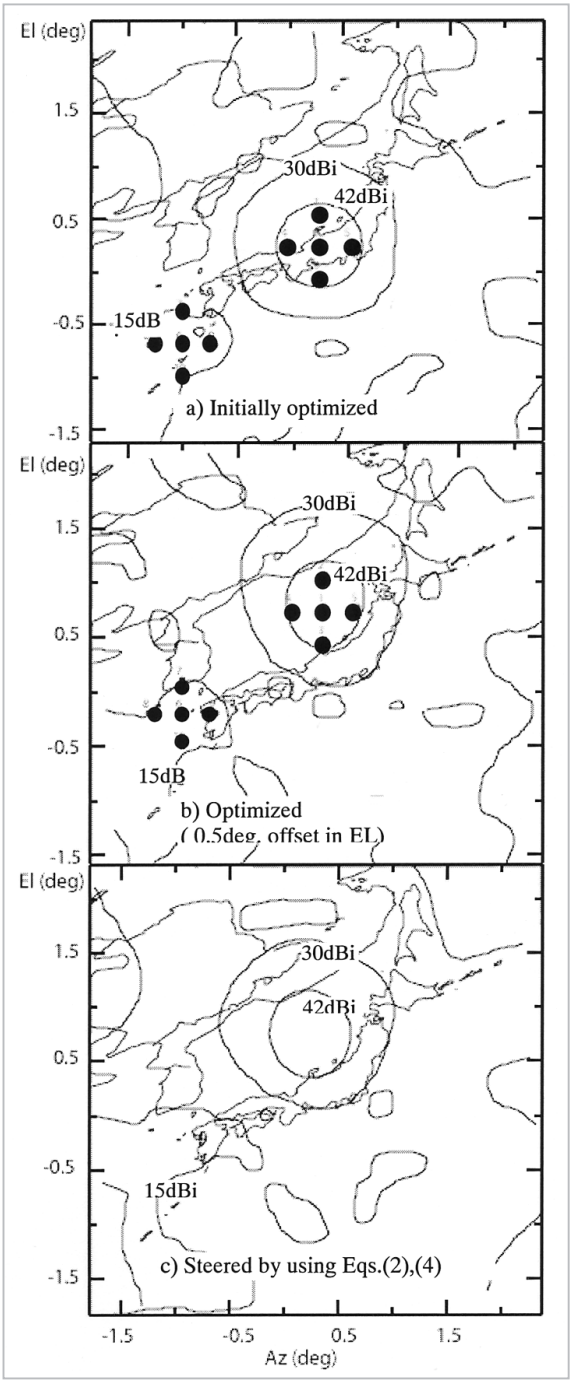

Fig.4 *Calculated transmitting antenna patterns. Marks in Figs. (a) and (b) indicate the gain constraint.*

Fig.5 shows the relationship between the desired scan angle (to the gain constraint point) and the steering angle obtained with Eq. (4). The steering angle from Eq. (4) and the desired scan angle are proportional with a ratio of 1:1.1. Nearly the same results were obtained for beam scanning from other initial beam positions.

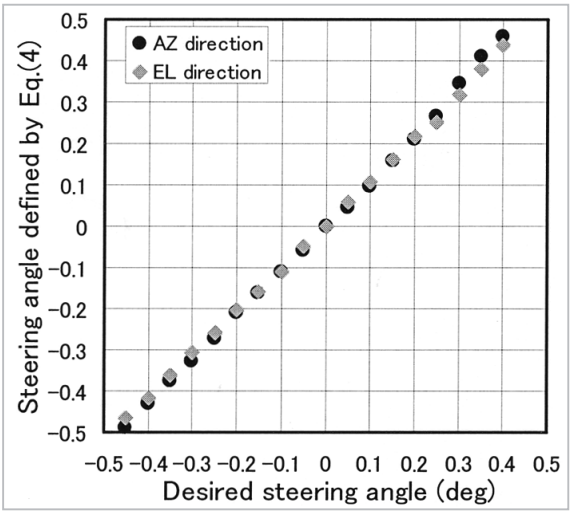

Fig.5 *Steering angle defined by Eq.(4) vs. desired steering angle.*

Fig.6 shows the relationship between rms phase deviation ε (defined by Eq. (3)) and the desired scan angle. Phase deviation ε increases with the scan angle, and becomes 12 to 22 degrees rms for a scan angle of 0.5 degrees. When a random phase error of this amount arises in the feed array, large degradation is expected, especially in terms of beam isolation [12]. The results shown in Fig.4c) correspond to the case of maximum phase deviation (in the +EL direction, with a scan angle of 0.5 degrees) shown in Fig.6. Significant degradation is not found in the scanned beam. Therefore, we conclude that phase deviation caused by the beam scanning method presented in this paper does not affect degradation of directivity to the same extent as random phase error having the same rms value.

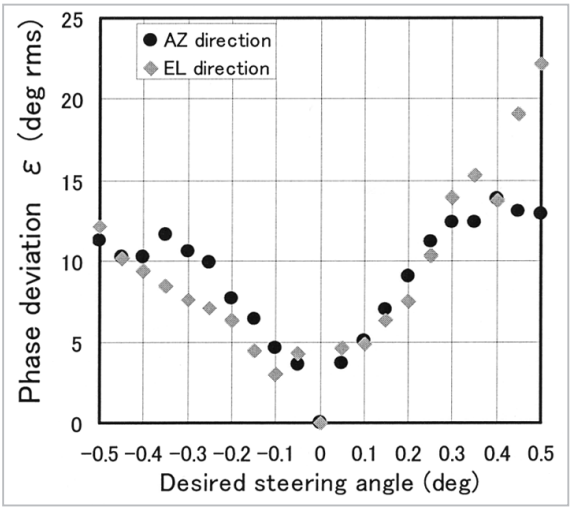

Fig.6 *Phase deviation ε vs. the desired steering angle.*

4 Development of onboard equipment

4.1 Beam-forming network 1

The structure of the transmitting BFN1 is shown in Fig.2. Beam port 1 corresponds to the independently controlled beam, and beam ports 2 and 3 correspond to the uniformly controlled beams. An input signal to the beam port is divided into thirty-one portions, which are subject to the required array weight (attenuation and phase sift) and amplification for subsequent output to the respective element ports. The attenuation and phase shift are performed by an MMIC active module in which a 5-bit variable attenuator, a 6-bit variable phase shifter, and an amplifier (to compensate for insertion loss) are integrated in a single package [13][14]. Table 1 shows the specifications of the module. Each MMIC module is mounted on a space-grade multilayer polyimide board. The MMIC modules are mounted on the front surface of the board with microstripe RF lines. On the rear surface, interface circuits between the MMIC modules and BFC are formed. Note that beam 2 uses MMIC modules that can be pre-set upon equipment startup so that the initial array weight can be modified. Table 2 shows the major specifications of the BFN1 (common to the transmitting BFN1 and to the receiving BFN1) and the specifications of the BFC.

Table 1 *Specifications of the active MMIC module for BFN1.*

Variable phase shifter	6-bit digital phase shifter
Phase error	< 2.8 deg. rms.
Variable attenuator	5-bit digital variable attenuator
Attenuation error	< 0.12 dB rms
Power consumption	< 150 mW
Minimum insertion loss	< 0.5 dB
VSWR	< 1.3
Dimensions and weight	13.0 x 27.2 x 3.5 (mm), 5 g

Table 2 *Specifications of Tx-BFN1 and BFC*

Excitation error	amplitude: < 0.4 dB rms., phase: < 6 dB rms
Weight	BFN1: < 15.2 kg, BFC: < 6kg
Dimensions	BFN1: 430 x 352 x 175 (mm), BFC: 292 x 224 x 188 (mm)
Power consumption	BFN1: < 50 W, BFC: < 12 W

4.2 Beam-forming controller

The beam-forming controller (BFC) calculates the array weight, controls the MMIC modules in the BFN, and interfaces with the telemetry and tracking control subsystem (TTC) of the satellite. Table 3 shows the operating modes and main functions of the BFC.

The test mode is used mainly to confirm the functions of the MMIC modules. In operating modes other than the test mode, the BFC provides amplitude and phase values for temperature compensation, based on the temperatures of several components of the feed sec-

Table 3 *Operating modes and functions of BFC*

Test mode	Array weight is controlled by sending the control bit patterns for each MMIC module. This mode is mainly applied to the device test of the MMIC modules.
Normal mode	Beam pointing is carried by sending an angle command(AZ, EL) for independently steerable antenna beams.
Program scan mode	A program data specifying the direction of beam pointing (AZ, EL) as a function of time is firstly set, then beam tracking is carried out based on the program data.
REV measurement mode	Excitation phase for an array element is rotated with a specified phase step and time interval. This mode enables array calibration with the REV method..
Onboard re-programming mode	This mode is used for updating the control software in BFC from ground station via the TTC link.

tion, and converts these values into control bit patterns for the MMIC modules. In this conversion, control bit pattern for a variable-attenuator is determined, to compensate the insertion loss of a variable phase shifter that is dependent on the phase shift. The determined bit patterns are buffered sequentially in the interface circuits of the MMIC modules in the BFN, and finally the settings of all the modules are updated simultaneously by an update command. The transition time during update is 10 ns or less, significantly shorter than the symbol duration of a signal. Therefore, beam pointing control is performed without interruption in communication link and without the inter-beam interference due to the deformation of the antenna beam during the above transition time.

The normal mode is used communication and broadcasting experiments. In this mode, phase control Eq.(2) enables independent scanning for beam 1 and uniform scanning for beam 2 and beam 3. Program scan mode runs these scanning operations repeatedly at intervals of 0.2 sec. This mode is used to evaluate antenna patterns in orbit and to simulate handover between beams in mobile communication experiments. Although the steering angle in Eq.(2) is based on the antenna coordinate system in Fig.3, it is more convenient in actual operation to denote east and north as AZ and EL, respectively, with reference to the satellite's nadir. Since the onboard antenna is installed on the satellite so that the boresight (+Z of the antenna coordinates) may point to the central part of the Japanese islands (135E, 34.67N), the BFC calculates phase shift by converting the coordinate. Moreover, the BFC also calculates the scan angle required to compensate for the attitude error extracted from the satellite's telemetry data.

The REV (rotating element electric field vector method [15]) measurement mode is used to evaluate the feed section in orbit. Since the REV method does not require phase measurement of a received signal, it is suitable for evaluation of satellite phased array antennas in orbit [16]. However, after the satellite is launched, time averaging of received signal amplitude is needed to improve the measurement accuracy; therefore, it is necessary to perform phase rotation at sufficient time intervals. The REV mode is convenient especially for such in-orbit evaluation, as the excitation phase of an arbitrary element can be rotated by a specified phase step at specified time intervals. The in-orbit programming mode is used in the event of a fault after launch or when modifying experimental functions of the BFC.

4.3 Evaluation of array weight control

In order to verify the onboard temperature compensation function, a thermal test was conducted for the beam-forming network and the beam-forming controller. During the test, weight error was measured by changing the component temperature. According to the results of the thermal test of a BFN without temperature compensation, when the temperature (in this case, the temperature of the base plate the component) rose from −10℃ to +40℃, the insertion loss increased by about 4 dB. On the contrary, the results with the compensation shown in Fig.7 show that variation in insertion loss with a temperature change from −10℃ to +40℃ was within 1 dB. Moreover, among the thirty-one elements, amplitude and phase deviations were 0.4 dBrms or less and 4 degrees or less, respectively, which clearly demonstrated the effectiveness of the temperature compensation function of the BFC.

5 Evaluation of beam-scanning performance

To verify the performance of a reflector antenna, measurement of secondary radiation

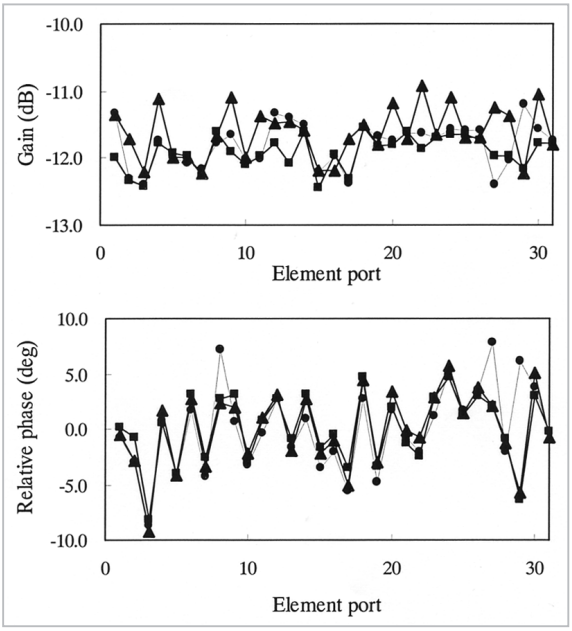

Fig.7 *Measured weight error of TX-BFN1. (a) Amplitude error, (b) Relative phase error*
●T=-10deg., ■T=22.5deg., ▲T=40deg.

patterns is generally the most direct way. However, it is difficult to measure the secondary pattern on the ground due to the influence of terrestrial gravity on the surface accuracy of the reflector, particularly given the reflector size of the ETS-VIII antenna (19 m in outer diameter). We therefore divided the verification process into two steps, as follows.

The first step involved evaluation using a BBM (breadboard model) for the BFN and the feed array. In this evaluation, the antenna reflector was not used. First, the primary electric field radiated by the feed array was measured by the near-field measurement method. Next, by assuming the shape of the antenna reflector (in this case, an ideally parabolic surface was assumed), electric-field distribution on the reflector surface was calculated, and then the secondary radiation pattern was evaluated [9]. Although in the BBM some of the structural parameters of the feed element, the excitation amplitude distribution, and the reflector structure were different from those of the flight model [9][17], the BBM is sufficient to verify the formation and pointing control of the antenna beams. Here it should be noted that the phase center of a cup MSA element is not on the feed patch but rather is located on the aperture plane of the metal cup, based on our measurement results. Therefore, the defocus distance is defined in terms of the distance from the reflector focal plane to the cup aperture plane.

Figs.8 a), b) show the estimated secondary radiation patterns with weights optimized for beam positions #3 and #4 shown in Fig.1, respectively. Figs.8 c), d) show patterns obtained with uniform scanning of these beams before and after the steering of -0.5 degrees in the AZ direction, respectively. The circles in the figure indicate desired beam positions before and after scanning, and dotted lines show measurement results as contour lines of 43, 42, and 20 dBi. The results of uniform scanning show that the desired scan angle was obtained, and that the required area gain (42 dBi) was obtained. Note that all of the 42-dBi contours are shifted from the desired positions by about 0.2 degrees toward the -AZ side. It is possible that this is attributable to alignment error in the feed array at the time of primary pattern measurement. On the other hand, although the specification for beam isolation (>20 dB) imposes a gain condition of 22 dBi or less in the areas of shared frequencies, the gain contour line of 20 dBi after the scan was slightly extended, indicating the presence of areas of deteriorated beam isolation. We conclude that this was caused by excitation error in the feed system and by the measurement errors in the primary radiation pattern, in addition to the phase deviation occurring through the beam scanning mentioned as shown in Fig.6.

In the next stage, secondary-pattern measurement was performed by combining an EM (engineering model) of the reflector and the major components of the feed section [18]. This measurement is intended (1) to confirm the total performance of the feed components in a configuration identical to that of the flight model, and (2) to verify the validity of antenna pattern evaluation based on the measured values of the geometrical shape of the reflector surface. The specifications and arrangement

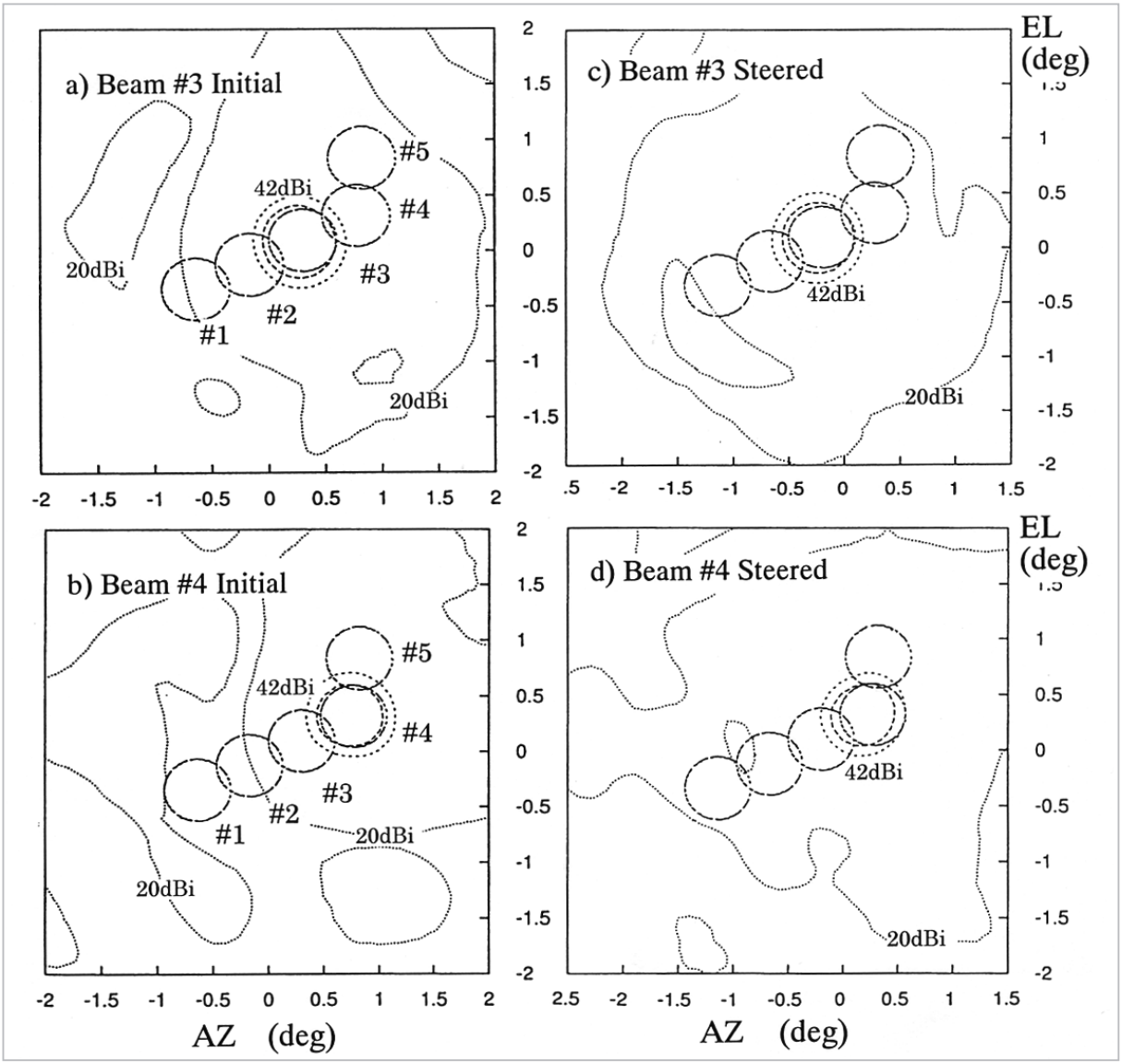

Fig.8 *Measured patterns before/after the steering of –0.5 degrees in AZ direction. Circles indicate the desired beam position.*

of the EM components used are basically the same as those of the flight components except that the large deployable reflector was constructed with only seven modules of the total fourteen modules to be used in the flight configuration due to the size constraints of the radio anechoic chamber.

The reflector shape was measured optically, then by combining the reflector with the feed section, the secondary radiation patterns were measured with near-field measurement method. The results of this measurement agree well with the predicted results based on the geometrical shape of the reflector surface [18]. Consequently, we conclude that the validity of the presented evaluation method of large reflector antennas has been demonstrated and that the performances of the feed system have also been verified.

6 Conclusion

This paper described the BFN1 and the BFC, both of which will be used in the phased-array-fed reflector antennas equipped on ETS-VIII satellite. We have shown that these devices have sufficient functions and performances to set the array weights for the formation and pointing control of the antenna beams.

References

1 E. H. Kopp, "Handheld telephony from geosynchronous orbit ", 17th ICSSC, AIAA-98-1396, 1998.

2 S. C. Taylor and A. R. Adiwoso, "The Asia cellular satellite system", 16th ICSSC, AIAA -96-1134, 1996.

3 Y. Kawakami, S. Yoshimoto, Y. Matsumoto, T. Ohira, and N. Hamamoto, "S-band Mobile satellite communications and multimedia broadcasting onboard equipments for ETS-VIII ", Trans. IEICE Vol. EB82-B, No. 7, pp.1659-1666, 1999.

4 K. Tokunaga, K. Ueno, Y. Matsumoto, Y. Suzuki, N. Hamamoto, and M. Okumura, "Design of phased array-fed reflector antennas for the Japanese Engineering Test Satellite 8 ", 50th International Astronautical Congress, IAF-99-M.3.06, 1999.

5 R. J. Mailloux, "Phased array theory and technology ", Proc. of the IEEE, Vol. 70, No.3, pp. 246-291, 1982.

6 Y. Matsumoto, Y. Hashimoto, T. Ide, M. Sakasai, N. Hamamoto, and M. Tanaka, "Beamformer with a single set of variable phase shifters for the pointing control of multibeam satellite antenna", Trans. IEICE, Vol. J80-B-II, No. 7, pp. 617-621, 1997.

7 T. Ohira, Y. Suzuki, H. Ogawa, and H. Kamitsuna, "Megalithic microwave signal processing for phased-array beamforming and steering ", IEEE Trans. Microwave Theory and Tech., Vol. 45, No. 12, pp. 2324-2332, 1997.

8 K. Nakamura, Y. Tsutsumi, K. Uchimaru, T. Tsujihata, and A. Meguro, "Large Deployable reflector on ETS-VIII ", 18th ICSSC, AIAA-98-1229, 1998.

9 K. Tokunaga, H. Tsunoda, Y. Matsumoto, and T. Ohira, "Electric design and prototype development of phased array feed for onboard reflector antennas", Trans. IEICE, Vol. J82 B, No. 7, pp. 1357-1365, 1999.

10 Y. Matsumoto, M. Tanaka, and M. Orikasa, "Development of cup-MSA feed array element for phased array satellite antennas", Trans. IEICE, Vol. J82 B, No. 7, pp. 1420-1424, 1999.

11 S. Hama, Y. Matsumoto, S. Taira "GEO based mobile communication of the near future -BFN and packet switch on the ETS-VIII-", Space Communications 15, PP. 55-63, 1998.

12 K. Tokunaga, H. Tunoda, Y. Matsumoto, and T. Ohira, "Feed development and secondary radiation characteristics of phased array fed reflector antennas for satellites", IEICE Technical Report, SANE97-65, 1997.

13 C. Sakakibara, H. Takasu, M. Okumura, S. Kamihashi, S. Hama, and Y. Matsumoto, "S-band MMIC phase shifter module for beam forming network ", IEICE 1998 General conference, C-2-37, 1998.

14 H. Takasu, C. Sakakibara, M. Okumura, S. Kamihashi, Y. Matsumoto, and S. Hama, "S-band MMIC active module with small phase variation and low insertion loss for beam forming network ", Trans. IEICE vol. E83-C, No. 1, pp. 122-125, 2000.

15 S. Mano and K. Katagi, "A method for measureing amplitude and phase of each radiating element of a phased array antenna", Trans. IEICE, Vol. J65-B, No. 5, pp. 555-560, 1982.

16 T. Tanaka, Y. Matsumoto, S. Yamamoto, K. Suzuki, and Y. Arimoto, "Antenna pattern measurement of S-band active phased array on ETS-VI ", Vol. J80 B-II, No.1, pp. 63-72, 1997.

17 Y. Matsumoto, T. Ide, M. Tanaka, T. Orikasa, and Y. Yamasa, "Array element and BFN design for phased-array-fed satellite antennas ", 17th AIAA International Communication Satellite Systems Conference, 98-1224, 1998.

18 K. Ueno, M. Atobe, A. Miyasaka, M. Orikasa, and M. Okumura, "Ground test of array-fed reflector antennas for ETS-VIII ", IEICE Technical Report, A・P2000-155 /SANE2000-136, 2001.

***MATSUMOTO Yasushi**, Dr. Eng.*

Associate Professor, Research Institute of Electrical Communication, Tohoku University (present Leader, Communication System EMC Group, Wireless Communications Division)

Wireless Communications

IDE Toshiyuki

Senior Researcher, Mobile Satellite Communications Group, Wireless Communications Division

Wireless Communications